

A Sensitivity Framework to Assess the Impact of Weather on Electric Power Networks

Arif Ahmed*, Fiona Stevens McFadden†, Ramesh Rayudu‡, and Tobias Massier§

*†Robinson Research Institute, *‡Smart Power and Renewable Energy Systems Group

*†‡School of Engineering and Computer Science, Victoria University of Wellington, Wellington 6140, New Zealand

*§TUMCREATE, 1 CREATE Way, #10-02 CREATE Tower, Singapore 138602

Email: *arif.ahmed@tum-create.edu.sg, †fiona.stevensmcfadden@vuw.ac.nz,

‡ramesh.rayudu@vuw.ac.nz, and §tobias.massier@tum-create.edu.sg

Abstract—This manuscript provides an analytical sensitivity framework to assess the impacts of individual weather parameters on conductor temperature and to determine the weather parameters that have greater potential to impact power networks and hence power system studies, which can be applied to any region around the globe. Application to weather parameter ranges possible across all of New Zealand (NZ) shows that the conductor temperature and hence the power network is most sensitive to the wind speed followed by the wind angle, and the solar irradiance, when paired with the ambient temperature. The sensitivity analysis framework is expected to aid utilities in assessing the region-specific impact of weather parameters on their network and hence improving their planning, operation, and analysis.

Index Terms—Weather Sensitivity, Heat Balance Equation, Impact assessment of weather, Power network impacts

I. INTRODUCTION

As power system technologies advance, accurate modelling has become crucial in understanding and analysing power systems.

Recently, methodologies and algorithms to incorporate weather into power system studies have been demonstrated and the importance of weather affecting power system analysis has been investigated [1]–[5]. Weather conditions impact greatly the power transfer capability and power losses of power networks [1]–[5]. The power loss error due to neglecting weather is observed to reach up to 30% and this error varies with varying weather and load conditions [2]. The weather-dependent power flow algorithm [3] demonstrates improvements in accuracy of power flow studies by explicitly considering weather conditions.

Weather mainly affects the conductor temperature and resistance of power networks, resulting in an impact on the power system states and subsequent analyses. Understanding of the temperature of the power network is important for utilities to maintain safe, reliable, and efficient operation of their networks. Some of the challenges faced by utilities include generation and substation expansion planning, network expansion planning, reactive power planning, active network management, etc. All of these are expected to benefit from identifying how and to what extent weather parameters impact temperature of power networks. As this will aid in planning, design, and operation of their various networks operating under diverse weather conditions.

Although various studies of the effects and impacts of weather conditions on power system studies are present, no systematic way of determining the impacts of individual weather parameters on the temperature of power network has been proposed. Therefore, this manuscript contributes by providing an analytical sensitivity framework to quantify the impacts of individual weather parameters on the conductor temperature of power networks and to determine the weather parameters that have greater impact potential, which can be applied to any region around the globe. Furthermore, this is then applied to an NZ weather scenario to determine the sensitivity of individual weather parameters on conductor temperature, which has also not been carried out in any way before.

Section II of the manuscript presents an overview of the conductor heat balance model utilised to derive the sensitivity framework. Section III presents the sensitivity framework and its derivation. An NZ case study of sensitivity analysis is undertaken in Section IV and the manuscript is concluded in Section V.

II. OVERVIEW OF CONDUCTOR HEAT BALANCE MODEL

The nonlinear heat balance model of an overhead conductor defines its heat equilibrium and relates its temperature, resistance, current, and the weather conditions surrounding it. It is well established in the power industry and mainly utilised for the purposes of thermal line rating of power conductors.

A. Steady-state Nonlinear Heat Balance Model

The steady-state nonlinear heat balance model is based on the assumption that the mean wind speed, wind direction, ambient temperature, solar radiation, and current is fairly constant and, hence, the conductor temperature does not change significantly.

The two established industry standards that define heat balance models are the IEEE Std 738TM-2012 [6] and the CIGRE Technical Brochure 207 (also known as Working Group 22.12) [7]. Although the same concept of heat balance is utilised, the approaches undertaken by the IEEE and CIGRE are different.

The steady-state nonlinear heat balance equation according to IEEE Std 738TM-2012 [6] is as follows:

$$q_c + q_r = q_s + q_j \quad (1)$$

In Eqn. (1), q_c is the heat loss rate due to convective cooling (in W/m), q_r is the heat loss rate due to radiative cooling

(in W/m), q_s is the heat gain rate due to solar radiation (in W/m), and q_j is the heat gain rate due to Joule heating (in W/m). The detailed equations for these can be referred to in the standards [6], [7], and Appendix A.

III. SENSITIVITY ANALYSIS FRAMEWORK

A schematic representation of the heat balance of a conductor is presented in Figure 1.

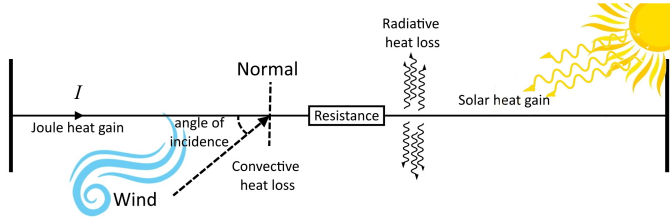


Fig. 1: Schematic representation of the heat balance of a conductor showing the heat losses and gains.

Heat balance of the conductor can be written as a nonlinear function of conductor resistance (R), ambient temperature (T_a), conductor temperature (T_c), absorptivity (α), solar irradiance (Q_s), conductor diameter (D_c), height of the conductor above sea level (H_e), wind speed (V_w), wind incidence angle (ϕ), emissivity (ε), and current (I) as follows:

$$f(R, T_a, T_c, \alpha, Q_s, D_c, H_e, V_w, \phi, \varepsilon, I) = q_r + q_c - q_s - q_j = 0 \quad (2)$$

The derivation of the sensitivity framework proceeds from Eqn. (2) yielding Eqn. (A.17) presented in the Appendix A.

To evaluate sensitivity for only weather parameters, Eqn. (A.17) is firstly simplified by excluding α , D_c , and ε . These are excluded based on the assumption that for any specific conductor, these conductor properties remain fairly constant compared to the varying weather conditions. The average height of a conductor above sea level (H_e) for a specific region also remains fairly constant and is, therefore, also neglected. As a result, Eqn. (A.17) is further simplified and rearranged to Eqn. (3) to make ΔT_c the subject such that the resulting expression is utilised to evaluate the sensitivities.

To obtain sensitivity coefficients relating to weather parameters (T_a , V_w , ϕ , and Q_s) only, Eqn. (3) is further simplified to Eqn. (4).

$$\Delta T_c = A\Delta T_a + B\Delta V_w + C\Delta\phi + D\Delta Q_s \quad (4)$$

Consequently, A, B, C, and D represent the change in conductor temperature due to a unit change in the respective weather parameter.

Eqn. (4) represents the sensitivity analysis framework to evaluate the sensitivity of conductor temperature to any weather parameter under any given loading and weather condition, for any region around the world.

IV. SENSITIVITY ANALYSIS FOR THE NEW ZEALAND CASE STUDY

Sensitivity analysis, in this case study, is performed by generating and investigating the contour plots of the sensitivity coefficients, which requires selection of a conductor and

different pairs of weather parameters. The 795 kcmil 26/7 Drake ACSR conductor [6] was selected in this sensitivity case study, which is an overhead conductor used in transmission and distribution systems. All pairs considered in the case study contain the ambient temperature (T_a) as it is found to be one of the important weather parameters in the extant literature [2], [8]. Consequently, the sensitivity coefficient A in Eqn. (4) is discarded and the pairs evaluated are (T_a, V_w), (T_a, ϕ), and (T_a, Q_s).

Table I presents the range and base value of the parameters required to evaluate the sensitivities¹. For each selected pair of weather parameters, a sweep over their ranges is performed. For example, to evaluate the sensitivity of conductor temperature (T_c) to a unit change in wind speed (V_w) (paired with the ambient temperature (T_a)), the conductor temperatures are firstly solved (Eqn. (2)) for all combinations of (T_a, V_w) pairs, while the rest of the parameters are fixed at their base values.

The sensitivity coefficients are then evaluated from Eqn. (4) and collected in relations, i.e., sets of ordered pairs, with the first element being the sweep value pair of the two weather parameters and the second element the calculated sensitivity. These relations are named **B**, **C**, and **D**, according to the second weather parameter (V_w, ϕ, Q_s) they refer to in Eqn. (4). For instance, the elements of relation **B** are of the form ($(T_{a_i}, V_{w_j}), B_{ij}$) representing the sensitivities as $\frac{\Delta T_c}{\Delta V_w}$.

TABLE I: Considered parameters

Parameter	Range	Base value
T_a (°C)	-5 to 35	13.2
Q_s (W/m ²)	0 to 1500	131
V_w (m/s)	1 to 25	3.51
ϕ (°)	0 to 90	59.96
I (A)	0 to 1500	750

A. Sensitivity due to V_w and T_a

Figure 2a presents the plot of T_c versus the variation in wind speed (V_w) and ambient temperature (T_a). The variation in V_w and T_a , the T_c varies from -1.6 °C to 58.6 °C. T_c is more sensitive to V_w at lower wind speeds and becomes quite insensitive beyond a certain threshold value. This is also evident in Figure 2b where the sensitivity coefficient relation **B** is presented for V_w versus T_a .

A sensitivity of -11.6 °C/m/s is found at the lowest wind speeds while as the wind speed increases the sensitivity decreases. This indicates that at lower wind speeds a unit change in V_w can cause a greater change in T_c by as much as 11.6 °C as presented in Figure 2b. However, as the wind speeds increase, the convective cooling effect saturates and the sensitivity drops to a very low level. Conductors operating in regions with varying wind speeds in the lower magnitudes are expected to experience the greatest impact of variations of convective cooling on conductor temperature. Therefore the impact of varying wind speed on power networks and their subsequent studies is expected to be greater.

¹Weather parameter ranges were selected to cover the entire spectrum of values that can be expected in NZ, while the weather parameter base values are averages for the year 2016 [9].

$$\Delta T_c = \frac{1}{\left(\frac{\partial q_c}{\partial T_c} + \frac{\partial q_r}{\partial T_c} - \frac{\partial q_j}{\partial T_c}\right)} \left[\frac{\partial q_j}{\partial R} \Delta R - \left(\frac{\partial q_c}{\partial T_a} + \frac{\partial q_r}{\partial T_a} \right) \Delta T_a + \frac{\partial q_s}{\partial Q_s} \Delta Q_s + \frac{\partial q_j}{\partial I} \Delta I - \frac{\partial q_c}{\partial \phi} \Delta \phi - \frac{\partial q_c}{\partial V_w} \Delta V_w \right] \quad (3)$$

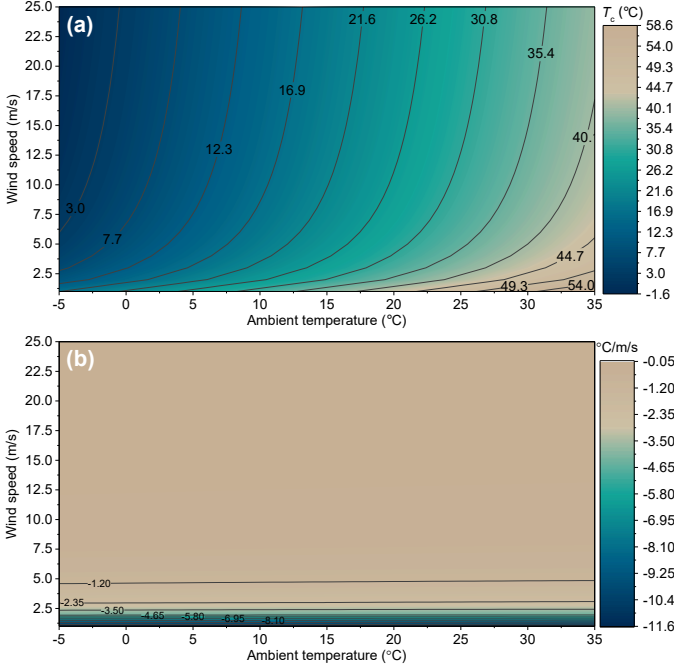


Fig. 2: (a) Contour plot of T_c for V_w vs T_a . (b) Contour plot of sensitivity coefficient relation B for V_w vs T_a .

B. Sensitivity due to ϕ and T_a

Figure 3a presents the plot of T_c versus the variation in wind incidence angle (ϕ) and ambient temperature (T_a). The variation in ϕ and T_a causes T_c to vary from 5 °C to 60.8 °C. The effects of ϕ observed is similar to V_w , as T_c is observed to be more sensitive at lower values of ϕ while at higher values of ϕ the sensitivity decreases.

Figure 3b presents the contour plot of the sensitivity coefficient relation C for ϕ versus T_a . There is high sensitivity as much as -0.686 °C/°, at lower angles which reduces to -0.022 °C/° at the highest ϕ of 90°. Similar to V_w , the incident wind angle's effect also saturates and the sensitivity drops in magnitude. This is observed approximately above 25°. As the incident wind angle, in general, is a highly variable parameter, it is also an important parameter impacting power networks.

C. Sensitivity due to Q_s and T_a

Figure 4a presents the contour plot of T_c versus the variation in solar irradiance (Q_s) and ambient temperature (T_a). T_c is observed to vary from 5 °C to 55.8 °C with the variation in Q_s and T_a . However, much of the conductor temperature range is due to the impact of the ambient temperature. There is an approximately constant sensitivity of the conductor temperature to each (Q_s and T_a), with the sensitivity to Q_s being roughly one-fifth of that to the T_a . The change in solar heat gain causes a lesser impact on T_c than that caused by a change in T_a .

Figure 4b presents the contour plot of sensitivity coefficient relation D for Q_s versus T_a , which also shows that the

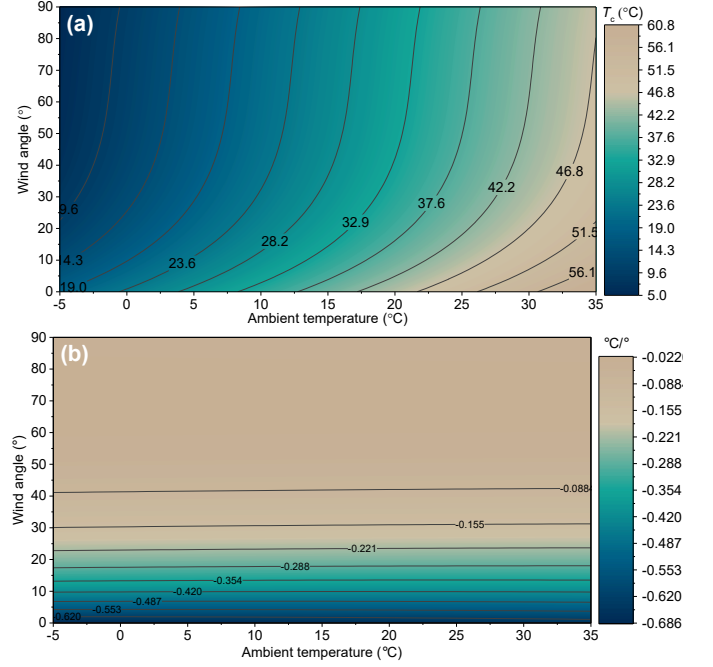


Fig. 3: (a) Contour plot of T_c for ϕ vs T_a . (b) Contour plot of sensitivity coefficient relation C for ϕ vs T_a .

sensitivity remains fairly constant from 0.0061 °C/W/m² to 0.0063 °C/W/m². This indicates lower impact of the variation of solar irradiance on the power network.

D. Summary and Discussion

The sensitivity case study undertaken gives a detailed analysis of the impacts that changes in ambient temperature paired with other weather parameters have on the conductor temperature for NZ. In addition, the sensitivity framework also calculates the minimum and maximum conductor temperature based on the ranges considered in the sensitivity case study. Consequently, this estimates the range of conductor temperature due to the range of weather parameters and weather conditions considered.

The highest range in conductor temperature was observed for the variation in wind speed paired with the ambient temperature. However, the maximum conductor temperature (60.8 °C) obtained was due to a 0° wind incidence angle. The sensitivity of the conductor temperature to variation in weather parameters was also observed to vary over the range of weather conditions. Table II summarises the largest and lowest per-unit sensitivities. The largest absolute sensitivity of 11.6 °C/m/s was at the lowest wind speed of 1 m/s and lowest ambient temperature of -5 °C while the lowest sensitivity was 0.0061 °C/W/m² at the lowest solar irradiance of 0 W/m² and lowest ambient temperature of -5 °C.

Although the weather parameter ranges assumed represent an NZ scenario, region-specific impacts can be easily evaluated

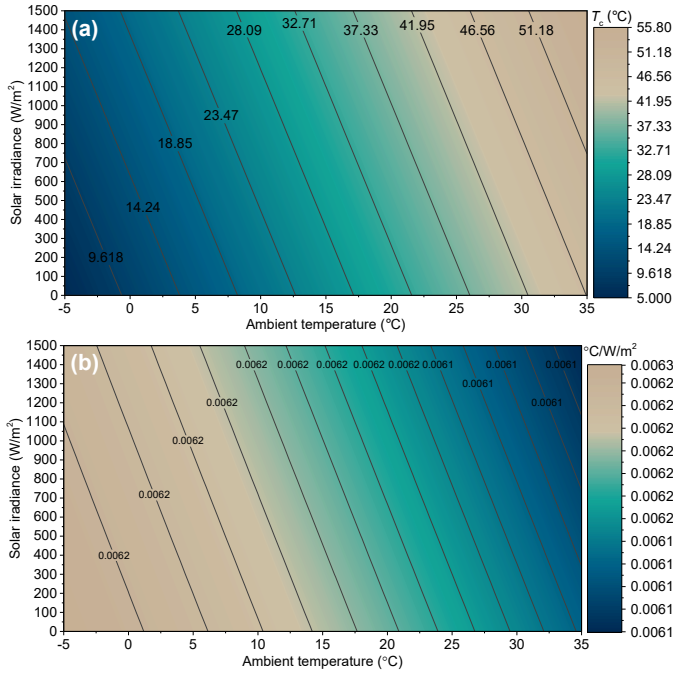


Fig. 4: (a) Contour plot of T_c for Q_s vs T_a . (b) Contour plot of sensitivity coefficient relation D for Q_s vs T_a .

TABLE II: Largest and lowest observed per-unit sensitivities

	T_a (-5 °C to 35 °C)		
	$\frac{\Delta T_c}{\Delta Q_s}$ ($\frac{^\circ\text{C}}{\text{W/m}^2}$)	$\frac{\Delta T_c}{\Delta \phi}$ ($\frac{^\circ\text{C}}{^\circ}$)	$\frac{\Delta T_c}{\Delta V_w}$ ($\frac{^\circ\text{C}}{\text{m/s}}$)
Largest	0.0063	-0.686	-11.6
Lowest	0.0061	-0.022	-0.05

using the sensitivity framework. This is important for utilities to generate helpful understanding of the impacts of weather parameters on their networks.

The sensitivity evaluated can be applied to approximate an indicative impact of the weather parameters on the power losses. For example, considering the largest absolute sensitivity of 11.6 °C/m/s (refer Table II), it can be estimated that a unit change in wind speed would cause approximately a 11.6 °C change in the conductor temperature, which would result in a total change of 20.4 MW in power losses for the 11,700 km network lines of NZ [10]. This is a massive change in power loss due to the impact of a single weather parameter. Therefore, for real networks operating under constantly changing loads and weather conditions, the impact of weather on the network becomes an important consideration for utilities.

In summary, the study presented gives an understanding of the impact of individual weather parameters on the conductor temperature for the possible weather conditions in NZ and presents a methodology to assess weather-related impacts for networks operating under various weather conditions. The sensitivity framework also aids in determining the possible temperature ranges of operating conductors in different regions based on region-specific weather conditions, which will help in the selection of appropriate network conductors by utilities. All of this is expected to aid region-specific power system planning, operation, and analysis by enabling understanding

of the weather-related effects on power networks.

V. CONCLUSION

This manuscript derives and presents a sensitivity analysis framework that is applicable for any region around the globe. The framework enables study of the impact of various weather parameters on power networks. An NZ case study is presented quantifying the sensitivity of conductor temperature to ambient temperature paired with other commonly measured weather parameters. The study indicates that power networks in NZ are highly sensitive to the wind speed and angle given the considered weather data. The study also highlights improvements in power loss estimates achievable by studying the weather-related impacts on networks. Consequently, the sensitivity framework is expected to aid utilities in understanding the impact of weather parameters on their power networks in order to improve planning, design, control, operation, and expansion of power grids.

ACKNOWLEDGMENT

This work was financially supported by the Singapore National Research Foundation under its Campus for Research Excellence And Technological Enterprise (CREATE) programme.

REFERENCES

- [1] V. Cecchi, M. Knudson, and K. Miu, "System impacts of temperature-dependent transmission line models," *IEEE Transactions on Power Delivery*, vol. 28, no. 4, pp. 2300–2308, Oct. 2013.
- [2] J. R. Santos, A. G. Exposito, and F. P. Sanchez, "Assessment of conductor thermal models for grid studies," *IET Generation, Transmission Distribution*, vol. 1, no. 1, pp. 155–161, Jan. 2007.
- [3] A. Ahmed, F. J. Stevens McFadden, and R. K. Rayudu, "Weather-dependent power flow algorithm for accurate power system analysis under variable weather conditions," *IEEE Transactions on Power Systems*, vol. 34, no. 4, pp. 2719–2729, July 2019.
- [4] A. Ahmed, F. S. McFadden, and R. Rayudu, "Transient stability study incorporating weather effects on conductors," in *2018 IEEE Power and Energy Society General Meeting (PESGM)*, Aug. 2018.
- [5] S. Frank, J. Sexauer, and S. Mohagheghi, "Temperature-dependent power flow," *IEEE Transactions on Power Systems*, vol. 28, no. 4, pp. 4007–4018, Nov. 2013.
- [6] "IEEE standard for calculating the current-temperature relationship of bare overhead conductors," *IEEE Std 738-2012*, pp. 1–72, Dec. 2013.
- [7] CIGRE Working Group 22.12, "Thermal behaviour of overhead conductors," *Technical Brochure 207*, 2002.
- [8] M. Bockarjova and G. Andersson, "Transmission line conductor temperature impact on state estimation accuracy," in *2007 IEEE Lausanne Power Tech*, July 2007, pp. 701–706.
- [9] "CliFlo: NIWA's National Climate Database on the Web," <http://cliflo.niwa.co.nz/>, Retrieved Feb. 2017.
- [10] Electricity Authority (2016), "Electricity in New Zealand," <https://www.ea.govt.nz/about-us/media-and-publications/electricity-new-zealand/>.

APPENDIX A

DERIVATION OF THE ANALYTICAL SENSITIVITY FRAMEWORK

Considering an initial state of equilibrium in Eqn. (2) and perturbing the parameters by a small amount, the expression is expanded applying Taylor series expansion with higher order terms neglected resulting in Eqn. (A.1). Eqn. (A.1) can now be rearranged to obtain the sensitivity of any desired parameter in relation to others by making it the subject of the equation.

$$\frac{\partial f}{\partial R} \Delta R + \frac{\partial f}{\partial T_a} \Delta T_a + \frac{\partial f}{\partial T_c} \Delta T_c + \frac{\partial f}{\partial \alpha} \Delta \alpha + \frac{\partial f}{\partial Q_s} \Delta Q_s + \frac{\partial f}{\partial D_c} \Delta D_c + \frac{\partial f}{\partial H_e} \Delta H_e + \frac{\partial f}{\partial V_w} \Delta V_w + \frac{\partial f}{\partial \phi} \Delta \phi + \frac{\partial f}{\partial \varepsilon} \Delta \varepsilon + \frac{\partial f}{\partial I} \Delta I = 0 \quad (\text{A.1})$$

Eqn. (A.1) acts as an essential expression that can be utilised to quantify the effect of any individual weather parameter on the conductor temperature for any conductor.

The partial differential expressions in Eqn. (A.1) are derived from the equations of q_r , q_c , q_s , and q_j (refer [6], [7]) as follows:

A. Partial Differentiation of q_r

The radiated heat loss expression q_r is:

$$q_r = \frac{17.8}{100^4} \varepsilon D_c [(T_s + 273)^4 - (T_a + 273)^4] \quad (\text{A.2})$$

Differentiating q_r with respect to R , α , Q_s , D_c , H_e , V_w , ϕ , and I yields 0. The remaining expressions are:

$$\frac{\partial q_r}{\partial T_c} = \frac{4 \cdot 17.8}{100^4} D_c \varepsilon (T_c + 273)^3 \quad (\text{A.3})$$

$$\frac{\partial q_r}{\partial T_a} = -\frac{4 \cdot 17.8}{100^4} D_c \varepsilon (T_a + 273)^3 \quad (\text{A.4})$$

$$\frac{\partial q_r}{\partial D_c} = \frac{17.8}{100^4} \varepsilon [(T_c + 273)^4 - (T_a + 273)^4] = \frac{q_r}{D_c} \quad (\text{A.5})$$

$$\frac{\partial q_r}{\partial \varepsilon} = \frac{17.8}{100^4} D_c [(T_c + 273)^4 - (T_a + 273)^4] = \frac{q_r}{\varepsilon} \quad (\text{A.6})$$

B. Partial Differentiation of q_c

The convective cooling expression q_c is represented by q_{c1} , q_{c2} , or q_{cn} in IEEE Std 738TM-2012 [6]. Only q_{c1} and its differentiation is presented here. q_{c2} , and q_{cn} can be similarly obtained. The expression for q_{c1} is:

$$q_{c1} = k_f K_{\text{angle}} [1.01 + 1.35 N_{\text{Re}}^{0.52}] (T_c - T_a) \quad (\text{A.7})$$

Differentiating q_{c1} with respect to R , α , ε , and I yields 0. Theremaining expressions are:

$$\begin{aligned} \frac{\partial q_{c1}}{\partial T_c} &= 1.01 K_{\text{angle}} [3.7385 \times 10^{-5} - 2.2035 \times 10^{-9} (T_c + T_a)] (T_c - T_a) \\ &+ 1.01 k_f K_{\text{angle}} \\ &+ 1.35 K_{\text{angle}} N_{\text{Re}}^{0.52} [3.7385 \times 10^{-5} - 2.2035 \times 10^{-9} (T_c + T_a)] (T_c - T_a) \\ &+ 0.351 k_f K_{\text{angle}} N_{\text{Re}}^{0.52} \left(\frac{T_c + T_a + 766.8}{2} \right)^{-1} (T_c - T_a) \\ &- 0.0012636 k_f K_{\text{angle}} N_{\text{Re}}^{0.52} [1 + 0.001835 (T_c + T_a)]^{-1} (T_c - T_a) \\ &- 0.5265 k_f K_{\text{angle}} N_{\text{Re}}^{0.52} \left(\frac{T_c + T_a + 546}{2} \right)^{-1} (T_c - T_a) \\ &+ 1.35 k_f K_{\text{angle}} N_{\text{Re}}^{0.52} \end{aligned} \quad (\text{A.8})$$

$$\begin{aligned} \frac{\partial q_{c1}}{\partial T_a} &= 1.01 K_{\text{angle}} [3.7385 \times 10^{-5} - 2.2035 \times 10^{-9} (T_c + T_a)] (T_c - T_a) \\ &- 1.01 k_f K_{\text{angle}} \\ &+ 1.35 K_{\text{angle}} N_{\text{Re}}^{0.52} [3.7385 \times 10^{-5} - 2.2035 \times 10^{-9} (T_c + T_a)] (T_c - T_a) \\ &+ 0.351 k_f K_{\text{angle}} N_{\text{Re}}^{0.52} \left(\frac{T_c + T_a + 766.8}{2} \right)^{-1} (T_c - T_a) \\ &- 0.0012636 k_f K_{\text{angle}} N_{\text{Re}}^{0.52} [1 + 0.001835 (T_c + T_a)]^{-1} (T_c - T_a) \\ &- 0.5265 k_f K_{\text{angle}} N_{\text{Re}}^{0.52} \left(\frac{T_c + T_a + 546}{2} \right)^{-1} (T_c - T_a) \\ &- 1.35 k_f K_{\text{angle}} N_{\text{Re}}^{0.52} \end{aligned} \quad (\text{A.9})$$

$$\frac{\partial q_{c1}}{\partial D_c} = 0.52 \cdot 1.35 k_f K_{\text{angle}} N_{\text{Re}}^{0.52} (T_c - T_a) D_c^{-1} \quad (\text{A.10})$$

$$\begin{aligned} \frac{\partial q_{c1}}{\partial H_e} &= 0.52 \cdot 1.35 k_f K_{\text{angle}} N_{\text{Re}}^{0.52} (T_c - T_a) (1.293 - 1.525 \times 10^{-4} H_e \\ &+ 6.379 \times 10^{-9} H_e^2)^{-1} (-1.525 \times 10^{-4} + 12.758 \times 10^{-9} H_e) \end{aligned} \quad (\text{A.11})$$

$$\frac{\partial q_{c1}}{\partial V_w} = 0.52 \cdot 1.35 k_f K_{\text{angle}} N_{\text{Re}}^{0.52} (T_c - T_a) V_w^{-1} \quad (\text{A.12})$$

$$\frac{\partial q_{c1}}{\partial \phi} = \frac{q_{c1}}{K_{\text{angle}}} [\sin(\phi) + 0.736 \cos(2\phi) - 0.776 \sin(\phi) \cos(\phi)] \quad (\text{A.13})$$

C. Partial Differentiation of q_s

In comparison to CIGRE standard, the IEEE Std 738TM-2012 [6] being the latter one has gone through much revision, is more simplistic, and is judged to be better suited for the purpose of this manuscript. On the other hand, the use of global solar irradiance data conforms better to the solar heat gain expression in the CIGRE [7] standard. As such, the solar heat gain expression from the CIGRE [7] standard is considered.

The solar heat gain expression q_s is:

$$q_s = \alpha D_c Q_s \quad (\text{A.14})$$

Differentiating q_s with respect to R , T_a , T_c , H_e , V_w , ϕ , ε , and I yields 0, while the remaining expressions are non zero. The remaining expressions are straightforward to calculate.

D. Partial Differentiation of q_j

The Joule heat gain expression q_j is:

$$q_j = I^2 R(T_c) \quad (\text{A.15})$$

Differentiating q_j with respect to T_a , α , Q_s , H_e , V_w , ϕ , and ε yields 0. The remaining expressions are also straightforward to derive. Only $\frac{\partial q_j}{\partial T_c}$ is presented. The expression for $R(T_c)$ should be referred to in the IEEE Std 738TM-2012 [6].

$$\frac{\partial q_j}{\partial T_c} = I^2 \left(\frac{R(T_{\text{high}}) - R(T_{\text{low}})}{T_{\text{high}} - T_{\text{low}}} \right) \quad (\text{A.16})$$

E. Overall Expression for Sensitivity Evaluation

All the partial derivative expressions when substituted in Eqn. (A.2) yield the ultimate sensitivity expression capable of evaluating multi-parameter/variable sensitivities. The resulting equation is as shown in Eqn. (A.17).

$$\begin{aligned} &-\frac{\partial q_j}{\partial R} \Delta R + \left(\frac{\partial q_c}{\partial T_a} + \frac{\partial q_r}{\partial T_a} \right) \Delta T_a + \left(\frac{\partial q_c}{\partial T_c} + \frac{\partial q_r}{\partial T_c} - \frac{\partial q_j}{\partial T_c} \right) \Delta T_c \\ &- \frac{\partial q_s}{\partial \alpha} \Delta \alpha - \frac{\partial q_s}{\partial Q_s} \Delta Q_s + \left(\frac{\partial q_r}{\partial D_c} + \frac{\partial q_c}{\partial D_c} - \frac{\partial q_s}{\partial D_c} \right) \Delta D_c \\ &+ \frac{\partial q_c}{\partial H_e} \Delta H_e + \frac{\partial q_c}{\partial V_w} \Delta V_w + \frac{\partial q_c}{\partial \phi} \Delta \phi + \frac{\partial q_r}{\partial \varepsilon} \Delta \varepsilon - \frac{\partial q_j}{\partial I} \Delta I = 0 \end{aligned} \quad (\text{A.17})$$

In Eqn. (A.17), the partial expression of q_c that corresponds to the largest convective heat rate yielding expression (from q_{c1} , q_{c2} , and q_{cn}) is considered.

Eqn. (A.17) enables the study of the sensitivity of conductor temperature to a per-unit change in all the other parameters and variables of the nonlinear heat balance model.